Research Article | Vol. 24, No. 20 | 03 Oct 2016 | OPTICS EXPRESS 22917

Optics EXPRESS

kW-class direct diode laser for sheet metal cutting based on DWDM of pump modules by use of ultra-steep dielectric filters

U. WITTE,[1,*] F. SCHNEIDER,[1] M. TRAUB,[1] D. HOFFMANN,[1] S. DROVS,[2] T. BRAND[2] AND A. UNGER[2]

[1]*Fraunhofer-Institute for Laser Technology, Steinbachstr. 15, 52074 Aachen, Germany*
[2]*DILAS Diodenlaser GmbH, Galileo-Galilei-Str. 10, 55129 Mainz-Hechtsheim, Germany*
[*]*ulrich.witte@ilt.fraunhofer.de*

Abstract: A direct diode laser was built with > 800 W output power at 940 nm to 980 nm. The radiation is coupled into a 100 µm fiber and the NA ex fiber is 0.17. The laser system is based on pump modules that are wavelength stabilized by VBGs. Dense and coarse wavelength multiplexing are realized with commercially available ultra-steep dielectric filters. The electro-optical efficiency is above 30%. Based on a detailed analysis of losses, an improved e-o-efficiency in the range of 40% to 45% is expected in the near future. System performance and reliability were demonstrated with sheet metal cutting tests on stainless steel with a thickness of 4.2 mm.

OCIS codes: (140.2020) Diode lasers; (140.2010) Diode laser arrays; (140.3298) Laser beam combining; (140.3390) Laser materials processing.

References and links

1. V. Krause, "Entwicklung der Leistung und des Wirkungsgrades von Diodenlasern höchster Leistung," presented at the 11th AKL – International Laser Technology Congress, Aachen, Germany, 27–29 Apr. 2016.
2. K. Price, S. Karlsen, P. Leisher, and R. Martinsen, "High-brightness fiber-coupled pump laser development," Proc. SPIE **7583**, 758308 (2010).
3. A. Siewert, "Multi-Core Fibre Lasers with High Performance and High Efficiency," presented at the 11th AKL – International Laser Technology Congress, Aachen, Germany, 27–29 Apr. 2016.
4. Datasheet, "e12-12-120-0976-3-105-0.22-SI-FPT-2.0-HT," (2016), http://www.nlight.net/nlight-files/file/DatasheetsV2/element/9xx/(e12_1200976105)%20e12-12-120-0976-3-105-0_22-SI-FPT-2_0-HT.pdf.
5. Datasheet, "976nm, 270W, 225µm Ø, Fiber-Coupled, Multi-Bar Module Based Conduction-Cooled, Tailored Mini-Bars," (2016), http://dilas.com/assets/media/products/DILAS_MMF_TBar_IS58_270W_976nm.pdf.
6. J. Skidmore, M. Peters, V. Rossin, J. Guo, Y. Xiao, J. Cheng, A. Shieh, R. Srinivasan, J. Singh, C. Wei, R. Duesterberg, J. J. Morehead, and E. Zucker, "Advances in high-power 9XXnm laser diodes for pumping fiber lasers," Proc. SPIE **9733**, 97330B (2016).
7. R. K. Huang, B. Chann, and J. D. Glenn, "Ultra-high brightness wavelength-stabilized kW-class fiber coupled diode laser," Proc. SPIE **7918**, 791810 (2011).
8. M. Wood, "Laser beam technology development and application," presented at the 7th Alta Brillanza Workshop, Milano, Italy, 24–25 Sep. 2015.
9. H. Zimer, M. Haas, S. Nagel, M. Ginter, S. Ried, S. Rauch, A. Killi, and S. Heinemann, "Spectrally stabilized and combined diode lasers," in *Proc.of IEEE Conf. on High Power Diode Lasers and Systems* (IEEE, 2015), pp. 31–32.
10. S. Heinemann, H. Fritsche, B. Kruschke, T. Schmidt, and W. Gries, "Compact high brightness diode laser emitting 500W from a 100µm fiber," Proc. SPIE **8605**, 86050Q (2013).
11. A. Unger, R. Uthoff, M. Stoiber, T. Brand, H. Kissel, B. Köhler, and J. Biesenbach, "Tailored bar concepts for 10mm-mrad fiber coupled modules scalable to kW-class direct diode lasers," Proc. SPIE **9348**, 934809 (2015).
12. D. Belforte, "Fiber laser revenues boost the 2013 laser market," J. Indust. Laser Sol. **29**(01), 6–9 (2014), http://www.industrial-lasers.com/articles/print/volume-29/issue-1/features/fiber-laser-revenues-boost-the-2013-laser-market.html.
13. G. C. Rodrigues, H. Vanhove, and J. R. Duflou, "Direct diode lasers for industrial laser cutting: A performance comparison with conventional fiber and CO2 technologies," J. Phys. Procedia **56**, 901–908 (2014).
14. http://www.bystronic.ch/de/produkte/laserschneidsysteme/ByLaser.php
15. Trumpf Brochure, "TruLaser: Cost-effective cutting through thick and thin," (2016), http://www.trumpf-machines.com/index.php?eID=tx_nawsecuredl&u=0&file=fileadmin/DAM/trumpf-

#270566 http://dx.doi.org/10.1364/OE.24.022917
Journal © 2016 Received 28 Jul 2016; revised 8 Sep 2016; accepted 8 Sep 2016; published 23 Sep 2016

Optics EXPRESS

machines.com/Produkte/Prospekte/TruLaser_04_2016_ENG.pdf&t=1465232907&hash=69efefb44829c48f3c5faeb85599d5c7.
16. P. Loosen, "High Power Diode Lasers," in *High-Power Diode Lasers: Fundamentals, Technology, Applications*, R. Diehl, ed. (Springer, 2000).
17. F. Ferrario, H. Fritsche, A. Grohe, T. Hagen, H. Kern, R. Koch, B. Kruschke, A. Reich, D. Sanftleben, R. Steger, T. Wallendorf, and W. Gries, "Building block diode laser concept for high brightness laser output in the kW range and its applications," Proc. SPIE **9733**, 97330G (2016).
18. P. Leisher, M. Reynolds, A. Brown, K. Kennedy, L. Bao, J. Wang, M. Grimshaw, M. DeVito, S. Karlsen, J. Small, C. Ebert, R. Martinsen, and J. Haden, "Reliability of high power diode laser systems based on single emitters," Proc. SPIE **7918**, 791802 (2011).
19. D. Bonsendorf, S. Schneider, J. Meinschien, and J. W. Tomm, "Reliability of high power laser diodes with external optical feedback," Proc. SPIE **9733**, 973302 (2016).
20. B. Leonhäuser, H. Kissel, J. W. Tomm, M. Hempel, A. Unger, and J. Biesenbach, "High-power diode lasers under external optical feedback," Proc. SPIE **9348**, 93480M (2015).
21. C. Wessling, M. Traub, D. Hoffmann, and R. Poprawe, "Dense wavelength multiplexing for a high power diode laser," Proc. SPIE **6104**, 61040O (2006).
22. Y. Kasai, S. Sakamoto, Y. Takahashi, K. Katagiri, Y. Yamagata, A. Sakamoto, and D. Tanaka, "High-brightness laser diode module over 300W with 100µm/Na 0.22 fiber," Proc. SPIE **9733**, 973309 (2016).
23. Laserline, „Technical data LDF," (2016), http://www.laserline.de/technische-daten-ldf.html.
24. R. K. Huang, B. Samson, B. Chann, B. Lochman, and P. Tayebati, "Recent progress on high-brightness kW-class direct diode lasers," in *Proc.of IEEE Conf. on High Power Diode Lasers and Systems* (IEEE, 2015), pp. 29–30.
25. U. Witte, M. Traub, A. Di Meo, M. Hamann, D. Rubel, S. Hengesbach, and D. Hoffmann, "Compact 35 µm fiber coupled diode laser module based on dense wavelength division multiplexing of NBA mini-bars," Proc. SPIE **9733**, 97330H (2016).
26. S. Hengesbach, S. Klein, C. Holly, U. Witte, M. Traub, and D. Hoffmann, "Simultaneous frequency stabilization and high-power dense wavelength division multiplexing (HP-DWDM) using an external cavity based on volume Bragg gratings (VBGs)," Proc. SPIE **9733**, 97330K (2016).
27. S. Hengesbach, C. Holly, N. Krauch, U. Witte, T. Westphalen, M. Traub, and D. Hoffmann, "High-power dense wavelength division multiplexing (HP-DWDM) of frequency stabilized 9xx diode laser bars with a channel spacing of 1.5 nm," Proc. SPIE **8965**, 89650C (2014).
28. B. Chann, A. K. Goyal, T. Y. Fan, A. Sanchez-Rubio, B. L. Volodin, and V. S. Ban, "Efficient, high-brightness wavelength-beam-combined commercial off-the-shelf diode stacks achieved by use of a wavelength-chirped volume Bragg grating," Opt. Lett. **31**(9), 1253–1255 (2006).
29. C. Holly, S. Hengesbach, M. Traub, and D. Hoffmann, "Simulation of spectral stabilization of high-power broad-area edge emitting semiconductor lasers," Opt. Express **21**(13), 15553–15567 (2013).
30. P. Unger, "Introduction to Power Diode Lasers," in *High-Power Diode Lasers: Fundamentals, Technology, Applications*, R. Diehl, ed. (Springer, 2000).
31. P. Crump, A. Pietrzak, F. Bugge, H. Wenzel, G. Erbert, and G. Tränkle, "975 nm high power diode lasers with high efficiency and narrow vertical far field enabled by low index quantum barrier," Appl. Phys. Lett. **96**(13), 131110 (2010).

1. Introduction

Fiber-coupled direct diode lasers are available with very high output power (e.g. up to 50 kW have been demonstrated by Laserline [1]). They offer a long life time (> 300,000 h demonstrated [2]) as well as the potential of low costs (< 10$/W) and high electro-optical (e-o) efficiency. Highest e-o efficiency of more than 60% (ex 105 µm) is available at 9xx nm [3]. Typically, for pump modules with > 100 W optical power, the e-o efficiency is in the range of 40% to 53% at the nominal current [4–6]. However, due to their limited beam quality, direct diode lasers are rarely used for applications that require high brightness laser systems (> 100 MW/(cm^2 sr)) like cutting, deep penetration welding, and selective laser melting of metals.

In order to further increase the brightness of high-power diode-laser systems, dense wavelength division multiplexing (DWDM) can be used; multiple emitters operating at individual wavelengths are combined using spectrally selective elements (surface gratings, dielectric filters, VBGs). For DWDM, in contrast to coarse wavelength multiplexing (CWM), each diode laser is spectrally stabilized by internal or external wavelength-selective feed-back in order to reduce the spectral spacing between the individual lasers (Fig. 1). Several companies and research groups have demonstrated different DWDM designs that potentially enable output powers in the kW range with beam parameter products of less than 10 mm

Optics EXPRESS

mrad (e.g. TeraDiode [7], JDSU/Amada [8], Trumpf [9], DPI/Fraunhofer CLT [10], DILAS [11]).

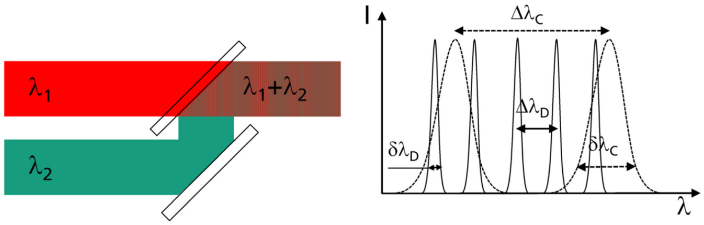

Fig. 1. Left: Principle of wavelength multiplexing. Right: Comparison of CWM (dotted) and DWDM (solid). The decreased spectral width $\delta\lambda$ enables a decreased spectral spacing $\Delta\lambda$. Hence more lasers can be multiplexed in the same wavelength interval (here 5 instead of 2).

Sheet metal cutting is one of the most important markets for manufacturers of high power laser systems [12]. The required output power ranges from approximately 500 W to 10 kW and the required beam parameter product from approximately 2 mm mrad to 22 mm mrad. Both depends strongly on the cutting process (oxygen assisted flame cutting of mild steel vs. nitrogen assisted fusion cutting of stainless steel), the material thickness and the required cutting quality [13]. Cutting machines for high quality cutting are usually equipped with 2 kW or more of optical output power [14,15] and a beam parameter product in the range of 4 mm mrad (c.f. Fig. 2). Due to the limited brightness of state of the art direct diode lasers, today's cutting machines are equipped with disk, fiber or CO_2 lasers [14,15].

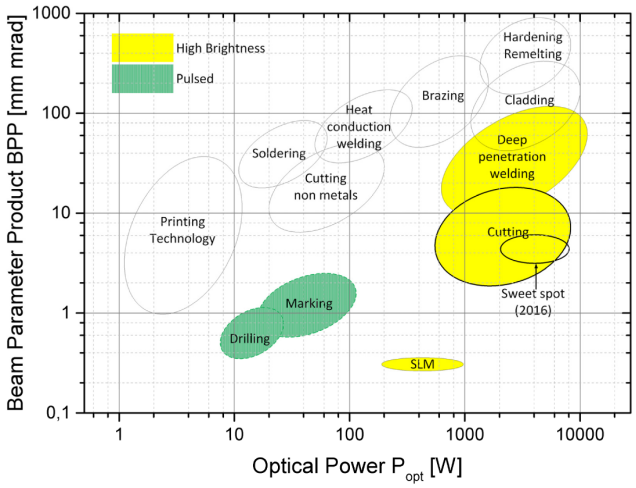

Fig. 2. Laser applications as a function of optical power and beam parameter product in 1998 [16]. The sweet spot indicates where standard machines are sold today by market leaders Bystronic and Trumpf [14,15].

Previously, sheet metal cutting by direct diode lasers was reported by several research groups [13] or diode laser manufacturers (e.g. TeraDiode [7], DPI [17]). None the less, the only systems with a high beam quality and a kW-class output power were demonstrated by TeraDiode and JDSU/Lumentum. The systems by TeraDiode is based on relatively large building blocks with long external resonators. Surface gratings are used for wavelength selective feedback. In this paper, we present an approach based on commercially available pump modules that are wavelength beam combined by use of dielectric filters. Experimental results obtained with a first breadboard set-up show the potential for high efficiency, compact size and low cost production. The output power and beam parameter product can be easily scaled to 2 kW and 6 mm mrad at an electro-optical efficiency above 40%.

Optics EXPRESS

2. State of the art diode laser modules

2.1 Lifetime

High power fiber coupled diode laser modules consist of a huge number of individual diodes. The impact of the number of diodes on the lifetime is described in [18]. Furthermore, lifetime of the chips might be influenced by the packaging – e.g. by back reflections or mounting induced stress. However, production of reliable modules without or with negligible packaging induced failures is possible and lifetimes of > 300,000 h have been demonstrated [2].

External wavelength stabilization can lead to a reduced lifetime which depends on the amount of optical feedback [19]. A high amount of optical feedback has been shown to lead to direct failure of the chip in some cases – especially at high drive currents [19,20]. However, with a reasonable low degree of back coupling – which corresponds to a reasonable low diffraction efficiency of the VBG – long lifetime is possible. On the one hand, a low front facet reflectivity can be needed in order to ensure a narrow spectrum with comparable low diffraction efficiency [21]. On the other hand, an increased front facet reflectivity can lead to higher tolerance against catastrophic optical mirror damage (COMD) caused by less filamentation [20]. Furthermore, the intensity distribution of the reflected light on the front facet has an impact on lifetime as well. Hence, research on how systems have to be designed in order to maintain the same lifetime as with unstabilized diode lasers is still ongoing. Up to now, there are only a few experimental studies published [20].

2.2 Brightness

Diode laser modules for pumping of fiber lasers are produced in high volume. Typically, the diode laser radiation is coupled into a fiber with a core diameter in the range of 105 µm to 220 µm. The highest brightness is published in [6] and [22] with 30 MW/(cm^2 sr) at 195 W optical output power and 23 MW/(cm^2 sr) at 300 W optical output power respectively. By employing CWM (c.f. Figure 1), the brightness can be further scaled. At least up to 88 MW/(cm^2 sr) corresponding to 20 mm mrad at an output power of 3.5 kW are commercially available [23]. In Fig. 3, examples for conventional (without wavelength stabilization technologies) high-power fiber-coupled diode laser systems are shown that were commercially available in 2015. Additionally, a fiber coupled diode laser system by TeraDiode [24] is plotted for reference. Above 1 kW output power, none of the conventional systems achieves a beam parameter product below 22 mm mrad.

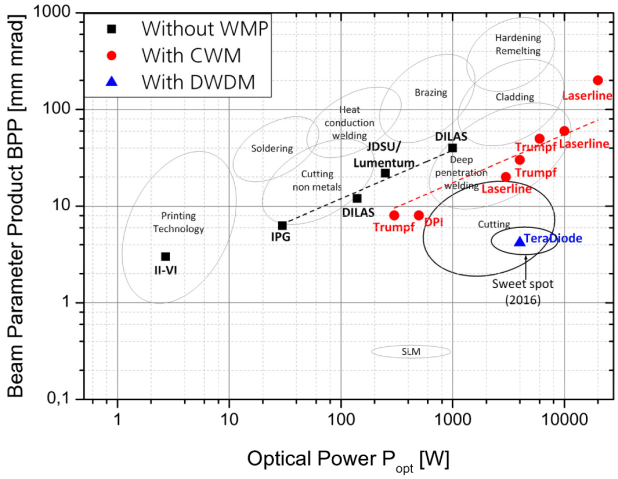

Fig. 3. Some commercially available high power fiber coupled diode lasers based on conventional spatial combining, coarse wavelength beam combining and DWDM (in 2015).

Optics EXPRESS

2.3 DWDM architectures

One well-known DWDM architecture for kW range diode lasers was invented by MIT and commercialized by TeraDiode. For instance, 4 kW ex 100 µm (NA ~0.08) are available with an electro-optical efficiency of 44% [24] corresponding to a brightness of approximately 2500 MW/(cm^2 sr). Several other companies and research groups have proposed alternative approaches (Table 1). One can distinguish between the optical elements that are used for wavelength multiplexing. Some concepts are based on simultaneous wavelength stabilization and multiplexing – i.e. the optical element(s) for multiplexing is placed inside the external resonator [26]. Others employ two steps for first wavelength stabilization and subsequent multiplexing. In the latter case, the elements used for wavelength stabilization can be distinguished. Additionally, the concepts differ from an economical point of view. If they are based on a platform for standard pumping modules that are produced in high volume, one can expect lower production costs. Production costs are also influenced by the diode package. With single emitters, a low thermal resistance per emitter (R_{th} ≈3 K/W) without micro-channel coolers can be achieved. Single-emitter based (sub-) systems are relatively tolerant against package induced stress and manufacturing tolerances of the optics. For bar-based (sub-) systems, the drive current is higher. On the other hand, systems based on diode laser bars are highly integrated as less individual optics and emitters are glued or soldered. Depending on the application, both approaches can be beneficial in terms of pricing. The submodules for this publication are based on mini-bars (5 emitters with 1 mm pitch compared to ~20 emitters with p ~0.5 mm) which offer a compromise between classical bars and single emitter.

Table 1. DWDM technologies - without any claim to completeness. "SE-based" indicates that the (sub-) modules are based on single emitters.

Institution	Multiplexing-element	Simult. λ-stab. & MP	Elements used for λ-stab.	λ-chirp on bar	Based on high volume architecture	Successful cutting tests published
TeraDiode [7]	surface grating	Y	-	Y	N	Y
ILT [25]	edge filters	N	DFB grating	Y	N	N
ILT [25]	edge filters	Y	-	Y	N	N
ILT [26]	VBGs	Y	-	SE based	N	N
ILT [27]	VBGs	N	VBGs	N	N	N
Trumpf [9]	surface grating	N	nodge filter	Y	N	N
DILAS [11]	edge filters	N	VBG	N	Y	N
DPI [10,17]	edge filters	N	VBG	SE based	N	N
MIT,PDLD [28]	surface grating	N	chirped VBG	Y	N	N
JDSU [8]	unknown	unknown	unknown	unknown	unknown	Y

Simultaneous wavelength stabilization and multiplexing can be advantageous – especially if a small spectral spacing $\Delta\lambda$ is required. The main advantages are as follows: (1) Less wavelength selective elements, (2) No beam-quality degradation occurs due to dispersion mismatch between the stabilization and the multiplexing elements (as seen in [9]), (3) In some cases, the diode lasers automatically emit longitudinal and transversal modes with minimum losses. This can lead to higher stability against detuning of the optics induced by

Optics EXPRESS

temperature changes or alignment tolerances [26]. On the other hand, these external cavities are generally longer and more complex, which can increase sensibility to mechanical and thermal instabilities. From our point of view, inherently cross-talk free concepts based on edge filters and high-volume pump module designs have the highest potential for low costs – at least in the short term.

3. Optics design

Our system consists of 6 free space diode laser modules manufactured by DILAS. The modules are based on the T-bar platform and equipped with newly developed narrow broad area diode laser mini bars that have a beam parameter product of approximately 7.5 mm mrad in the slow axis (SA) direction [19]. Each module is equipped with up to 9 bars that are wavelength stabilized by use of a single VBG. The radiation of three modules is then wavelength beam combined (DWDM) by use of ultra-steep dielectric filters. Subsequently, the radiation field is polarization coupled in order to reduce the beam parameter product in direction of the SA. The exit window of each module is imaged onto the polarization coupler in order to compensate for the optical path between the exit window and the polarization coupler. As a third step, two submodules – one operating at 97x nm and the other at 94x nm – are wavelength combined by use of dielectric filters (CWM). A Galilean telescope adapts the beam diameter between the SA and the fast axis (FA). The radiation is coupled into a commercially available fiber (QBH standard) with 100 µm core diameter and an NA of 0.2 by use of an aspheric lens. A schematic diagram and a ray tracing model of the demonstrator are presented in Fig. 4. All optical parts are mounted with commercial off- the-shelf mounts.

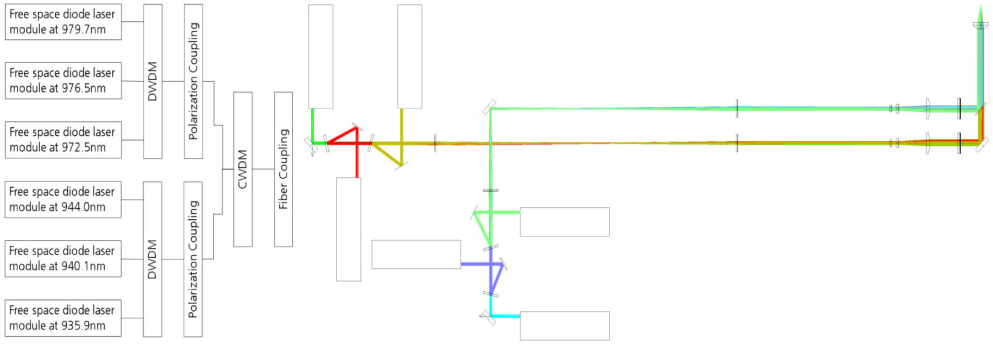

Fig. 4. Left: Schematic combining scheme. Right: Ray-tracing model.

4. Experimental results

In the following section, detailed results are presented for the modules operating at the center wavelengths λ_C of 944 nm, 940 nm and 936 nm; comparable results were obtained with the modules lasing around 976 nm.

4.1 Module characterization

Each module is equipped with a distinct VBG that determines its peak wavelength. However, side modes in the spectrum can occur and increase the spectral width. This depends on the ratio of power that is coupled back into the waveguide and on the mismatch between the gain maximum and the Bragg-wavelength [29]. The exact behavior is unknown as it depends at least on the front facet reflectivity and the chip design. In order to decrease the spectral width of the individual beam sources, the temperature of the cooling water is adapted for each module. The gain maximum of the diode lasers is estimated by the center wavelength of the free-running lasers. The center-wavelength shift with temperature amounts to 0.3 nm/K being in line with the literature [30]. When changing the cooling water temperature, the Bragg-wavelength of the VBG can shift as well. However, the temperature dependent Bragg-

Optics EXPRESS

wavelength shift is negligible for this application as it is in the range of 5 pm/K to 20 pm/K [27]. Although a high operating temperature may decrease losses at low operating currents, it can lead to increased losses at high operating currents due to a reduced e-o efficiency.

The VBGs integrated into each diode laser submodule have a red-shift compared to the gain maximum of the diodes. At 19°C cooling water temperature, the center wavelength λ_C for the free-running emitters increases from 927 nm at an injection current I of 2.5 A to 933 nm at 30 A (Fig. 5, right). Hence, the maximum red shift occurs for the VBGs with the largest Bragg-wavelength. Therefore the 2 modules lasing at the larger wavelengths (stabilized to 940 nm and 944 nm) require an increased temperature of the cooling water of 30°C and 50°C respectively. The modules lasing at 976 nm and at 980 nm are both operated at 30°C, and the module lasing at 972 nm is operated at 19°C.

At the operating point, all modules are well stabilized. Nearly 100% of the emitted power is encircled between the band edges $\lambda_{BE,i}$ ($T(\lambda_{BE,i})$ = 50%) of the filters (left (black) axis in Fig. 6, right). The encircled power is defined as:

$$\chi_{PC} = \frac{\int_{\lambda_{BE,1}}^{\lambda_{BE,2}} I(\lambda)\,d\lambda}{\int_{\infty}^{\infty} I(\lambda)\,d\lambda}. \tag{1}$$

High operating temperature, losses due to wavelength stabilization of diode lasers with standard front facet coating and on overfilling of the numerical aperture of the micro lens array for slow axis collimation (SAC array) at high operating currents lead to a reduction of the electro-optical efficiency and the maximum output power. In Fig. 6, left, the optical output power and e-o-efficiency are plotted for two different modules. Maximum power is obtained at 971 nm with 257 W at 35 A. The radiation is linearly polarized and wavelength stabilized. At an injection current of 25 A, the e-o efficiency is 57%. In [19], the e-o efficiency for a baseplate of 7 bars is 62% without wavelength stabilization and without housing. Hence, approximately 8% power losses occur that are mainly caused by wavelength stabilization and partly by integration into a housing and an increased stacking density in the FA (9 bars instead of 7). The cooling temperature of 50°C for the module at 944 nm decreases the optical power by 14% at 30 A.

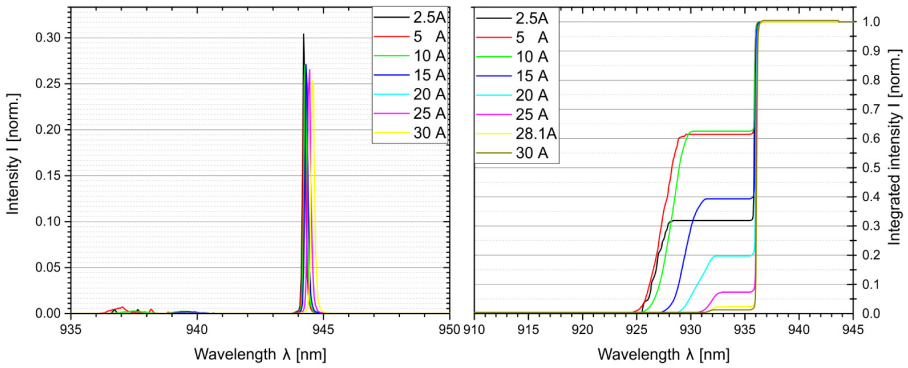

Fig. 5. Left: Spectrum of 944 nm submodule for different operating currents with cooling water temperature of 50°C. Right: Integrated intensity (power content) of 936 nm submodule operated at 19°C cooling water temperature.

Optics EXPRESS

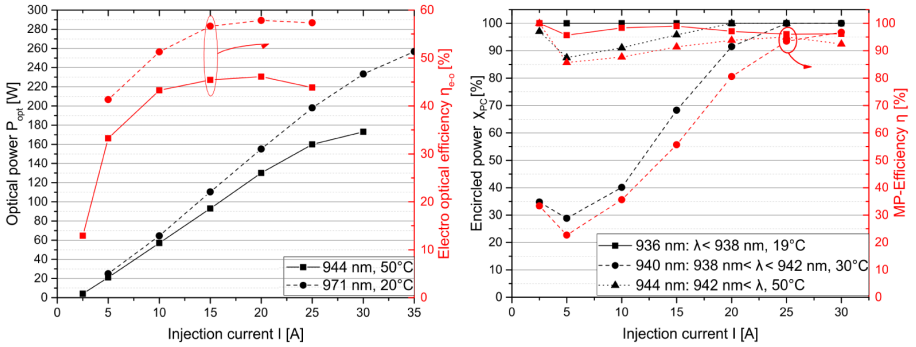

Fig. 6. Left: Optical output power and electro optical efficiency for 2 different diode laser modules. Right: Correlation between the energy that is encircled between the band edges of the corresponding filters and the multiplexing efficiency. The relatively low efficiency for the 940 nm submodule at low operating currents can be clearly attributed to side lobes in the spectrum.

4.2 DWDM efficiency

The multiplexing efficiency η_{MP} is defined as

$$\eta_{MP} = \frac{P_{MP}}{\sum P_{module,i}}. \quad (2)$$

with the power $P_{module,i}$ emitted by module i and the power P_{MP} in the wavelength combined beam. A multiplexing efficiency of approximately 95% at the operating point (25 A) was achieved for the modules at 936 nm, 940 nm and 944 nm. At lower injection currents, relatively high losses occur for the module that emits at a center wavelength of 940 nm due to side lobes in the spectrum (Fig. 6, right). A multiplexing efficiency of 91% was achieved for the 3 modules at 97x nm at the operating point of 30 A.

The filters are specified for $\eta_{MP} > 95\%$ for infinitesimal narrow spectra. Characterization of the actual filters (performed by the manufacturer) revealed that up to 96.7% is possible. Hence, less than 2% losses occurred due to alignment tolerances, side lobes in the spectra and depolarization of the diodes.

4.3 Efficiency of polarization coupling

The maximum polarization coupling efficiency η_{PC} amounts to 91% and drops down to 86% for high injection currents (Fig. 7, left). It is defined as the ratio of the power $P_{bef,PC}$ measured directly behind the polarization coupler and the power $P_{beh,PC}$ measured directly before the coupler.

The efficiency can be limited by (1) depolarization of the diode laser radiation, (2) overfilling of the clear aperture of the coupler, (3) wavelength mismatch between the diode laser radiation and the coupler and (4) thermal effects. The polarization coupler consist of a beam splitter and a waveplate which is relatively sensitive to a wavelength mismatch. However, a direct characterization of the individual parts is impossible, as the polarization coupler is manufactured as a monolithic element. The coupler is designed for a center wavelength of 940 nm with a spectral width of ± 5 nm and an angular acceptance of ± 3°. The dielectric filters are designed for s-polarized radiation; the transmittance and reflectance depend strongly on the polarization. P-polarized radiation emitted by the modules lasing around 936 nm and 940 nm would be transmitted at the corresponding filters and decrease the multiplexing efficiency. The degree of polarization (DoP) of the pump modules χ_{PM} decreases the maximum multiplexing efficiency $\eta_{MP,max}$ by [25]:

Optics EXPRESS

$$\eta_{\mathrm{MP},\chi} = \eta_{\mathrm{MP,max}} \cdot \left(\chi + \frac{1-\chi_{\mathrm{MP}}}{N} \right). \tag{3}$$

N describes the number of beam sources and equals to 3.

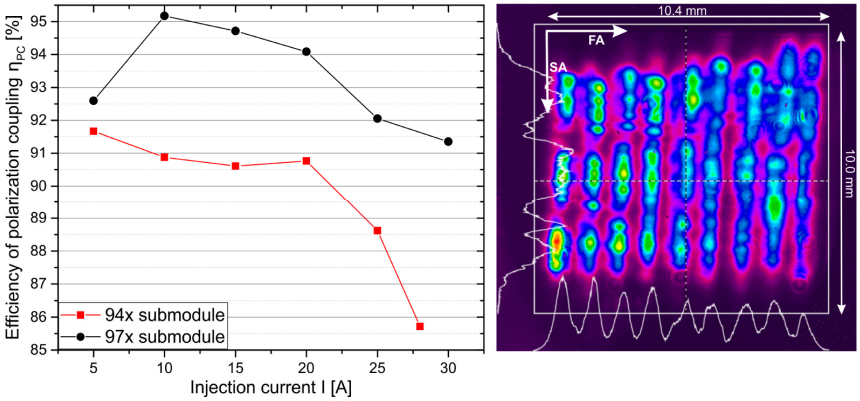

Fig. 7. Left: Efficiency of polarization coupling. Right: Intensity distribution after polarization coupler and beam shaping.

Based on the high multiplexing efficiency of 95%, we conclude that the DoP is approximately 97% for the pump modules and at least 98% for the multiplexed radiation. The beam diameter is relatively independent of the injection current. The spectral width of the radiation decreases towards high injection currents (Fig. 5, right). This indicates that the design wavelength of the polarization coupler is detuned by thermal effects. In principle, the design wavelength can be tuned by adjusting the angle of incidence which has not yet be done.

4.4 CWM efficiency

The efficiency of coarse wavelength multiplexing η_{CWM} is defined as the ratio of the power $P_{\mathrm{beh,PC}}$ measured behind the polarization coupler and the power $P_{\mathrm{beh,CWM}}$ measured behind the CWM-mirror (last element before the aspheric lens for fiber coupling, c.f. Figure 4, right):

$$\eta_{CWM} = \frac{P_{beh,PC}}{P_{\mathrm{beh,CWM}}}. \tag{4}$$

Hence, it includes losses at the beam shaping unit that symmetrizes the beam radius after the polarization coupling. The efficiency of coarse wavelength multiplexing amounts to η_{CWM} = 93% and to η_{CWM} = 95% for the branch around the center wavelength of 976 nm and for the branch around the center wavelength of 940 nm respectively.

4.5 Fiber coupling and electro-optical efficiency

The fiber coupling efficiency η_{FC} is 88% at the operating current for the 94x nm submodule only:

$$\eta_{FC} = \frac{P_{\mathrm{ex100\mu m}}}{P_{\mathrm{beh,CWM}}}. \tag{5}$$

$P_{\mathrm{beh,CWM}}$ indicates the power measured before the focusing optics. This is very close to commercially available pump modules without dense wavelength multiplexing. Typical values for commercial products are in the range of 90%. However, when the fiber position is optimized for the 97x nm subsystem, coupling efficiency for the 94x nm submodule drops by

Optics EXPRESS

10% (Fig. 8, left). This indicates alignment errors of the filter for CWM and leads to a reduction of the system efficiency of approximately 5%.

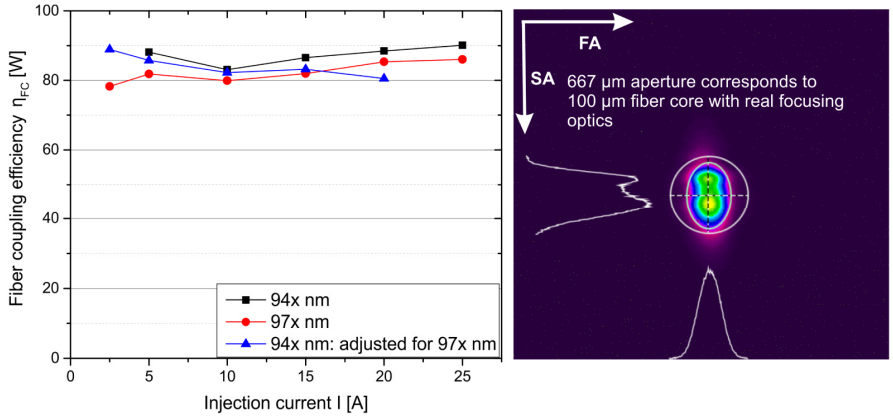

Fig. 8. Left: Fiber coupling efficiency. Right: Intensity distribution in focal plane.

The optical to optical (opt-opt) efficiency $\eta_{\text{opt-opt}}$ is defined as the ratio of the power measured at the fiber exit $P_{\text{ex100µm}}$ and the sum of the power emitted by the 6 individual diode laser modules P_{module}:

$$\eta_{opt-opt} = \frac{P_{\text{ex100µm}}}{\sum_{i=1}^{6} P_{i,\text{module}}}. \tag{6}$$

The opt-opt efficiency is limited to 65% at the working point (Fig. 9, left). The numerical aperture (NA) ex fiber is 0.17 for 86% power content. Figure 8, right indicates that the focus diameter in the FA can be increased by approximately 25% without leading to additional coupling losses. Hence, the NA can be decreased by adapting the Galilean telescope.

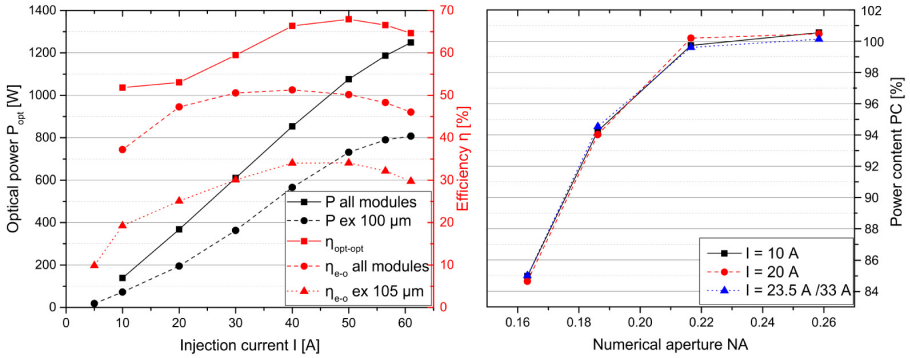

Fig. 9. Left: Optical power and efficiencies ($\eta_{\text{e-o}}$: electro-optical; $\eta_{\text{opt-opt}}$: optical to optical) for the final kW-demonstrator. The injection current is the sum of the injection currents for the two individual controllable subunits (94x nm and 97x nm). Right: Power content against NA.

5. Summary of loss mechanisms

The wavelength multiplexing efficiency is 95% for 3 nearly commercial modules and close to the limit for the applied filters. None the less, the opt-opt efficiency of this first laboratory set-up is limited to 65%. The main loss mechanisms are – as described in detail in section 4:

- Polarization coupling: 10%

Optics EXPRESS

- Alignment tolerances for CWM-mirror that reduce the fiber coupling efficiency: 5%
- At low currents: side lobes in the spectrum
- CWM: 4%
- DWDM of the modules around the center wavelength of 976 nm: 3%

Consequently, one can mitigate these loss mechanisms with the following improvements:

- Rotational alignment of polarization coupler in conjunction with mounts that enable an improved cooling of the monolithic element
- Mount for the CWM-mirror that enables precision and stable alignment
- Choice of VBGs with Bragg-wavelengths close to the gain maximum of the diode lasers
- Alignment of the AOI onto the CWM-mirror and increasing the spectral spacing between the 940 nm branch and the 976 nm branch by suppression of side lobes at the center wavelength of 972 nm
- Improved control of the cooling water temperature

Additionally, the e-o efficiency and output power P of the modules is reduced by increased cooling water temperature due to the mismatch between Bragg-wavelength and gain maximum (c.f. subsection "module characterization") and by use of VBGs with high diffraction efficiency. We expect that, in average, the output power of the modules can be increased by 10%. As shown in Fig. 10 and in [21], in general, the spectral width can be significantly reduced for external cavities by applying tailored AR-coatings to the front facet instead of using VBGs with high diffraction efficiency. None the less, as described in section 2, this can also influence life time, beam quality and sensitivity to back reflections.

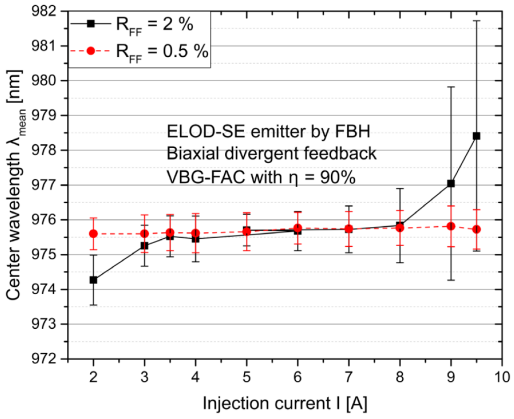

Fig. 10. Center wavelength and spectral width for 95% power content (error bars) for two externally stabilized single emitters with different front facet coatings. The epitaxial design of the single emitters (SE) was optimized for external wavelength stabilization with an "extremely low divergence" (ELOD) in the vertical axis of 30° (95% PC) [31]. A monolithic VBG-FAC is used for stabilization.

6. Sheet metal cutting tests

The diode laser system (Fig. 11) was integrated into a cutting system. The cutting head is mounted on a gantry robot system (Reis RLP 16). The cutting head (Laserfact F2-Y) is equipped with a collimator with a focal length of 120 mm and a focusing optics with a focal length of 220 mm. Stainless steel (1.4301) was successfully cut (Fig. 12, right) with thicknesses t between 0.8 mm and 4.3 mm. Standard parameters for cutting with 1 µm fiber

Optics EXPRESS

lasers were used (nozzle diameter 2 mm, nozzle stand-off 0.7 mm, N_2 cutting-gas pressure 12 bar).

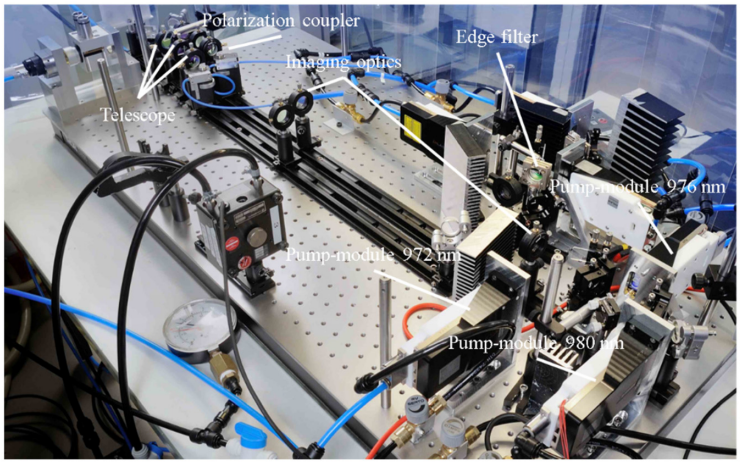

Fig. 11. Laboratory diode laser system on a breadboard in mobile flow-box for cutting experiments. The pump modules are manufactured by DILAS.

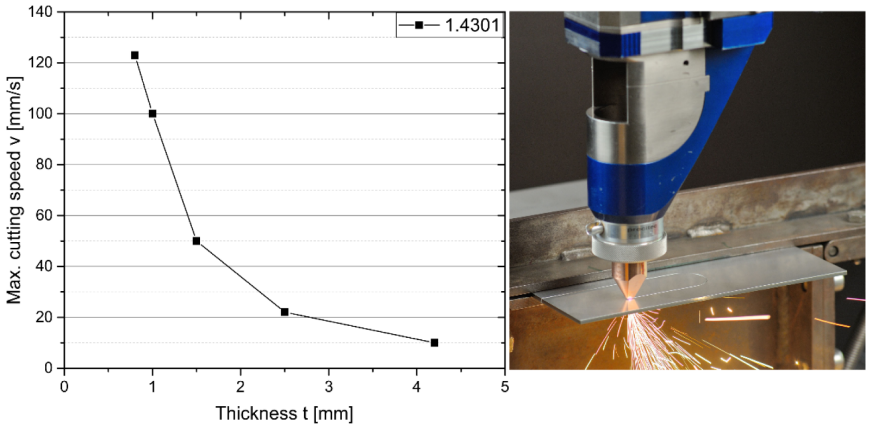

Fig. 12. Left: Maximum cutting speed as a function of the material thickness for stainless steel. Right: Sheet metal cutting experiment (stainless steel, d = 2.5 mm, v = 18 mm/s, nozzle diameter d_n = 2 mm, nozzle distance d = 0.5 mm, N_2 gas pressure p = 12 bar). The optical power at the work piece is 630 W. 16% power losses occur in the optics due to an overfilling of the NA (≈6%) and AR-coatings for 1070 nm (≈10%) as a standard cutting head for fiber lasers are used.

The focus position was adjusted by measuring the cut kerf width dependent on the focus position. In thin section fusion cutting, the smallest kerf width is reached when the focus is positioned at the top side of the sheet. This is also the focus position for maximum speed. For a more tolerant working point, the focus position for the cutting speed variation in 1 mm thickness was set to –0.5 mm, the middle of the sheet.

Samples with a thickness of 0.8 mm were cut with a speed of up to 123 mm/s. Maximum cutting speed for a sample thickness of 4.2 mm decreases to 10 mm/s (Fig. 12, left).

The roughness for samples with 1 mm thickness was approximately Rz = 20 µm and relatively independent of the cutting speed. However, the burr depends significantly on the process parameters. For optimized cutting speed (80 mm/s ≤ v ≤ 90 mm/s), the cuts were almost burr-free (burr < 0.01 mm). The burr increased to more than 0.08 mm for speeds down to 50 mm/s since no power modulation was used to avoid burr in the low speed regime. In

Optics EXPRESS

Fig. 13, two cut edges are shown with a thickness of 1 mm and 2.5 mm respectively. The cutting speed was optimized for minimum burr. The cutting quality is therefore comparable to the quality achieved with fiber lasers which corresponds to results presented in other publications [8].

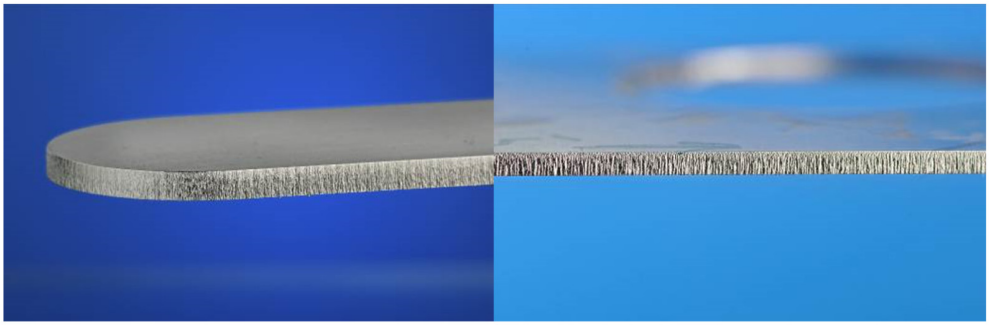

Fig. 13. Cut edge for 2.5 mm (left) and 1 mm (right) stainless steel.

7. Summary and conclusion

The direct diode laser system has been tested successfully for sheet metal cutting and enables optical output powers above 800 W in combination with a brightness of approximately 100 MW/(cm^2 sr). Compared to other kW-class direct diode lasers with 100 µm fibers, the external resonator is relatively short (L_{Res} ~100 mm compared to L_{Res} > 1000 mm [9]), the submodules are based on a state of the art pump module architecture (T-bar concept manufactured by DILAS) and the elements used for DWDM (dielectric filters) are comparable cheap. Hence, an economic production is feasible.

However, the optical to optical efficiency of this first laboratory experimental set-up is limited to approximately 65% which is significantly lower than the Stokes efficiency of a fiber laser (>86%). The two main reasons are the limited efficiency of polarization coupling (~90% instead of 98% as possible) and alignment tolerances (~5%). Furthermore, the high operating temperature of 4 modules reduced the e-o efficiency by approximately 5 to 10%. We have shown that the system is suited for optical to optical efficiencies in the range of 80% and an e-o efficiency in the range of 45%. The NA and the foot print can be significantly decreased by use of tailored optics for the telescope and the polarization coupling in combination with tailored mounts that are more compact than conventional mounts.

Funding

This work was funded in part by the European Commission (EC) within the BRIDLE project in the seventh framework program under grant number 314719 (www.bridle.eu).

Acknowledgments

We thank our project partners for assistance and fruitful discussions.